Applied Chemical Engineering (2026) Volume 9 Issue 4 ISSN: 2578-2010 (O)
doi: 10.59429/ace.v9i4.6006

RESEARCH ARTICLE

Design of a novel Schiff base ligand and some of its metal complexes, and DFT/NBO Study; evaluation of the biological activity of a copper (II) complex as an anti-colon cancer agent

Thanaa Abdul Ameer Hilal [1], Zainab Jasim Mohammed [2], Mohammed Noaman alanssari [1,*], Hanan Faleh Mohsein [1], Nadia Ezzat Al-kirbasee [1,3]

[1] *Department of Chemistry, College of Education for Women, University of Kufa, Najaf, Iraq*

[2] *Al- Kufa Secondary School for Distinguished Students, General Directorate of Education of Najaf Al-Ashraf, Ministry of Education, Iraq*

[3] *College of Engineering, University of Warith Al-Anbiyaa, Karbala, Iraq*

***Corresponding author:** Mohammed Noaman alanssari, mohammedn.alanssari@uokufa.edu.iq

ABSTRACT

In this study, a new heterocyclic Schiff base ligand was synthesized from 4-aminobenzamide and indoline-2,3-dione, followed by the preparation of its Cu (II), Zn (II), and Co (II) complexes. The prepared compounds were characterized with the use of different spectroscopic methods, such as FTIR, UV-Vis, 1HNMR, 13CNMR, the melting point determination, and the molar conductivity measurements. The findings indicated that the ligand is a bidentate ligand with nitrogen and oxygen donor atoms to form octahedral metal complexes. The biological activity of the copper (II) complex was tested against human colon cancer cells (HCT116) and normal cells (HDF). The complex had a great inhibitory effect against the cancer cell proliferation, as confirmed by the IC50 values. This shows that the compound under study can be developed in future to be used for pharmaceutical applications. Moreover, the electronic properties of the copper complex were studied by Density Functional Theory (DFT) calculations. The HOMO-LUMO, ELF and NBO analyses revealed the good electronic stability, charge transfer behavior and electron localization around the donor atoms. The findings offer theoretical insight into the electronic characteristics, charge-transfer behavior, and stability of the prepared copper complex, thus facilitating the experimental characterization and biological assessment.

Keywords: Schiff base, copper complex, 4-aminobenzamide, colon cancer, HDF, density functional theory, HOMO–LUMO, NBO analysis, ELF analysis

ARTICLE INFO

Received: 7 May 2026
Accepted: 31 August 2026
Available online: 02 November 2026

COPYRIGHT

Copyright © 2026 by author(s).
Applied Chemical Engineering is published by Arts and Science Press Pte. Ltd. This work is licensed under the Creative Commons Attribution-NonCommercial 4.0 International License (CC BY 4.0).
https://creativecommons.org/licenses/by/4.0/

1. Introduction

Because of their many uses as well as ease of synthesis, Schiff's base compounds have attracted a lot of interest [1]. These kinds of compounds can be produced in a lab as well as found in nature [2]. Schiff bases, or Azomethines (-C=N-), are a substantial class of compounds characterized by a carbon-nitrogen double bond, distinguishing them from other organic compounds [3]. Schiff bases are synthesized through the condensation of primary amines with ketones or aldehydes [4]. The heterocycles of Schiff base compounds are a representative class of molecules that have at least one atom other than carbon within the structure of the aromatic rings. Among the most common heteroatoms are nitrogen, oxygen, and sulfur, whereas rings composed of other elements have also been shown to work well [5-7].

The ability of such compounds to function as ligands and

to coordinate with various metal ions to form stable metal complexes has attracted attention [8]. Interestingly, adding transition-metal ions to the Schiff bases broadens their applications across many industries. These uses include agrochemicals, fungicides, the dye and food industries, analytical chemistry, and catalysis [9]. Additionally, these metal complexes could decrease the cytotoxicity of both metal ions and original Schiff bases, while concurrently increasing the biological activities related to Schiff bases [10-13]. Because of their versatility in coordinating with metal ions, including nickel, copper, zinc, and cobalt, through different donor atoms, such as oxygen (O) and nitrogen (N), Schiff base ligands are of special importance.

Numerous biological processes, including antioxidant activity as shown in earlier research [14,15], are facilitated by this flexibility. The biological activities include anticancer [16], antibacterial [17], antifungal [18], and catalytic [19]. The function of metal ions in promoting cell membrane permeation as well as the interaction with biomolecules [20] is responsible for the complexes' increased activities in comparison with free ligands. The synthesis and characterization of a new heterocyclic Schiff's base compound, as well as many of its complexes, and an investigation related to the biological activity of the prepared copper complex, were the objectives of the presented work. In addition to the experimental synthesis and spectroscopic characterization, computational studies can provide a deeper understanding of the electronic behavior of Schiff base metal complexes [21,22]. In addition to the experimental synthesis and spectroscopic characterization, computational studies can provide a deeper understanding of the electronic behavior of Schiff base metal complexes. Therefore, in this study, Density Functional Theory (DFT) calculations were used to support the structural interpretation of the copper complex and to examine its electronic properties [23,24]. To determine the electron distribution, donor-acceptor interactions, the charge-transfer behavior, and the stability of the complex, HOMO-LUMO [25], ELF [26], and NBO analyses were used [27]. This computational part helps in explaining the coordination behavior of the copper complex and its possible uses in catalysis and materials chemistry [28].

2. Experimental Section

2.1. Materials

The materials used in this study are indoline-2,3-dione, 4-aminobenzamide, and silver nitrate, which were purchased from Sigma-Aldrich (England). $CoCl_2 \cdot 6H_2O$, $ZnCl_2$, $CuCl_2 \cdot 2H_2O$, ethanol, methanol, and glacial acetic acid were from B.D.H Company. Benzene was obtained from G.C.C. Company, while hydrogen tetrachloroaurate(III) trihydrate was obtained from Glentham Life Sciences. Ethanol absolute was from Sharlut Company. Dimethyl sulfoxide (DMSO) was purchased from A.C.S. Company. All these chemicals were used without further purification, as supplied.

2.2. Instrumentation

Melting point measurements for the ligand and its complexes were done using an electrothermal 9300 melting point LTD from the UK. Proton nuclear magnetic resonance spectra were acquired as solutions in DMSO-d6 by applying 500 MHz to a Varian spectrometer. For UV-visible spectra, a Shimadzu UV-1700 dual-beam spectrophotometer was used.

Carbon spectra (13C-NMR) have been recorded on a Bruker spectrometer at 75 MHz with the use of DMSO-d6 as solvent, and FTIR spectra were taken utilizing a Shimadzu FTIR 8400 spectrometer employing KBr particles in the 4000–400 $cm^{-}1$ wavelength range the Digital Conductivity Series Ino.Lab.720 device has been used to test the molar conductivity of the prepared chelated complex solutions, which are dissolved in the DMSO solvent. Deep freezer (−800oC) from Marubeni, Japan, cell culture incubator (Memmert, Germany), distillatory Ogawa Seiki (Japan), cooling centrifuge (Beckman Model J2-21, USA), ELISA reader (Organon Teknika), drying and sterilization oven (Hermle, Germany), multiwall plate, inverted microscope (Leica, Germany), microtiter plate, and 96-well plate from the USA were utilized. The

vacuum pump (Leitz, Germany), water bath (Memmert, Germany), 0.22 µm Millipore filter (Sartorius, Germany), sterile tissue culture flasks (25.75 cm2) (Nunc, Denmark), and pH meter (LKB, Sweden) were used.

2.3. Preparation of the Schiff base ligand

After adding 10 mmol of carbonyl compound indoline-2,3-dione to a 100 Ml round-bottom flask equipped with a stopper and condenser, two drops of glacial acetic acid as well as 20 Ml of 100% ethanol were added as catalysts. With continuous stirring, the mixture was gradually supplemented with 20 Ml of primary amine (4-aminobenzamide) diluted in 20 mL of absolute ethanol (Fig. 1). When specified, the mixture was refluxed. After that, the mixture was allowed to cool to room temperature. Precipitates formed when some of the solvent evaporated under lower pressure. After filtering, cleaning, and proper treatment, the precipitate recrystallized. The fundamental physical characteristics regarding Schiff bases and the ideal fabrication conditions are displayed in Fig. 1 and Table 1.

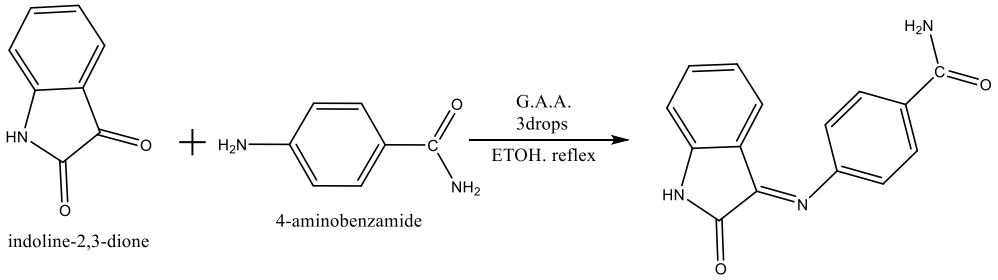


Figure 1. Structure of the ligand

2.4. Preparation of complexes

Anhydrous Zn (II) chloride and ethanolic solutions of Cu (II) and Co (II) hydrated metal chloride are added to the ligand that is dissolved in the solvent in molar ratios of 1:2 (metal: ligand). After filtering off the residual solids, 5 Ml of heated 50% ethanol was used to wash away any remaining unreacted starting materials. After being air-dried and recrystallized from ethanol, they were then refluxed with stirring for at least half an hour, and colored precipitates formed at room temperature before their percentage was calculated.

In vitro cell cytotoxicity and viability assays: Development of a colon cancer cell line (HCT116 cells).

2.5. Cancer cell lines and cell cultures.

The human colorectal cancer cell line HCT-116 and the normal cell line HDF (Human Dermal Fibroblast) were supplied by the National Cell Bank of Iran (Pasteur Institute, Iran). In addition, the cells HAVE BEEN grown in RPMI1640 (Gibco) containing FBS (10%) and antibiotics (100 µg/Ml streptomycin and 100 U/Ml penicillin). The cells have been maintained at 37° Celsius in humidified air with CO2 (5%) and passed through PBS solution and trypsin/EDTA (Gibco).

MTT cell viability assay. Cell growth as well as viability have been assessed by utilizing the MTT [3-(4, 5-dimethylthiazol-2-yl)-2, 5-diphenyltetrazolium Bromide] (Sigma-Aldrich) test. In short, the cells were digested with trypsin, harvested, and seeded into 96-well plates with 200 µl of fresh medium per well for 24 hours after being adjusted to a density of 1.4 × 10^4 cells/well. Following formation of a monolayer of cells, they are exposed to a 600- 7.4 µg/Ml DMSO solution containing the compounds for 24 hours at 37 degrees Celsius in CO2 (5%). Following treatment, 200µl/well of MTT solution (0.50mg/Ml in PBS) has been added, and the plate has been incubated for four more hours at 37°C, and the monolayer culture has still

been present in the original plate. MTT solution: Following the removal of the cell supernatant, 100.0µl of dimethyl sulfoxide has been added to each well. Until all of the crystals are dissolved, the cells have been shaken at a temperature of 37 °C. Cell viability was measured by absorbance at 570nm using an ELISA reader (Model Wave XS-2, BioTek, USA). The concentration of compounds that resulted in 50% cell death (IC50) was determined using relevant dose-response curves.

3. Results and Discussion

3.1. Characterization of ligand and its metal complexes

The color of the Schiff base ligand's chelate complexes varied depending on the metal ions, despite the ligand being yellow semi-crystals. The ligand, as well as its complexes, was insoluble in water and quite air-stable. However, they yield stable solutions at room temperature when dissolved in the common organic solvents, such as ethanol, methanol, chloroform, acetone, and pyridine. Nonetheless, Table 1 provides certain analytical and physical data.

Table 1. Physical Characteristics of Compounds

Compounds	Color	M.Wt.	Melting point ^{0}C	Yield (%)
L	yellow	265	170-172	%80
$[Co(L)_2Cl_2]$	Green- brown	659	258-dec.	%85
$[Cu(L)_2Cl_2]$	brown	664	228-230	%82
$[Zn(L)_2Cl_2)]$	orange	666	237-dec.	%85

3.2. Infrared Spectral Studies

In coordination chemistry, infrared spectroscopy is often used to evaluate changes in absorption bands of active groups within the ligand molecule before and after coordination. In the present investigation, we used potassium bromide (KBr) tablets to record infrared spectra of the organic ligand and its Cu(II), Zn(II), and Co(II) chelate complexes in the 400–4000 cm^{-1} range. The shape, location, and intensity of absorption bands that corresponded to the active groups have been observed.

The ν(N–H) stretching vibration is responsible for the medium as well as the broad band observed in the ligand's infrared spectrum at approximately 3184 cm^{-1}. This band's position is maintained at almost the same frequency in metal complexes' spectra, which could be indicated by nonparticipation in the complex [29]. Also, the complexes' and ligand's spectra showed medium-broad bands at (3103-3062) cm^{-1}, which were attributed to ω (C-H) aromatic, and bands at (3007-2879) cm^{-1}, which have been attributed to Σ (C-H) aliphatic [30]. The carbonyl group (C=O) was responsible for the ligand spectrum's absorption band at 1674 cm-1, which also appeared in the complexes' spectra at frequencies between 1664 and 1660 cm^{-1} [31].

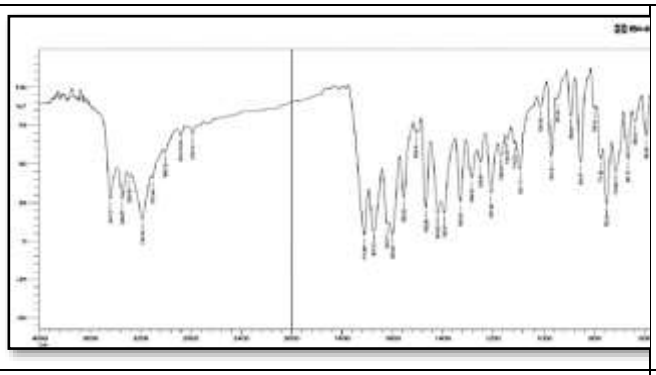
Coordination through such groups with metal samples is suggested by this shift towards lower frequencies as well as changes in the bands' shape and intensity [32]. The azomethine group ν (-C=N-) was represented by the ligand's absorption band at a frequency of 1620 cm-1 [33]. This band has been seen in the complex spectra at frequencies of (1612-1608) cm^{-1}. It underwent noticeable changes in intensity and shape, as well as shifts towards lower frequencies, indicating that the azomethine group (C=N) is involved in coordination with the metal ions. The complexes' spectra showed weak absorption bands for (M-O) and (M-N) groups at frequencies of (466-462) and (503-491) cm^{-1}, respectively.

Through the designated coordination sites, these bands show how the metal ions and the ligand are coordinated [34, 35]. The frequencies are absent from the ligand spectrum, suggesting that these groups facilitate coordination with metal ions. The IR spectrum data above indicate that the ligand acts as a neutral bidentate chelating agent. The nitrogen atom of the azomethine group, as well as the oxygen atom of the

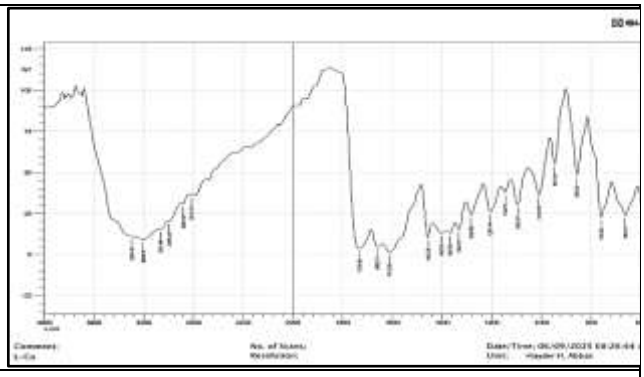
carbonyl group in the heterocyclic form, forms the coordination sites, creating a five-membered chelate ring. Table (2) shows the most significant absorption bands in the infrared spectra of the ligand and resulting complexes.

Table 2. Infra-red spectral data (cm^{-1}) of the ligand and its complexes

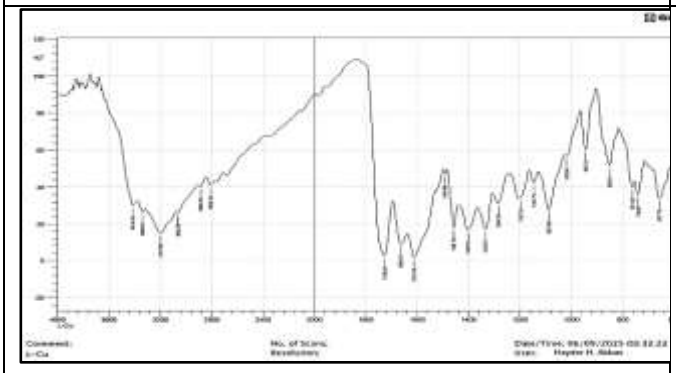
Compounds	N-H	C-H arom.	C-H aliph.	C=O	C=N	C-N	M-N	M-O
L=Ligand	3184	3103	2879	1674	1620	1207	…	…
$[Co(L)_2Cl_2]$	3203	3064	2995	1660	1612	1207	503	466
$[Cu(L)_2Cl_2]$	3197	3062	2885	1664	1612	1204	503	466
$[Zn(L)_2Cl_2]$	3207	3080	3007	1660	1608	1209	491	462



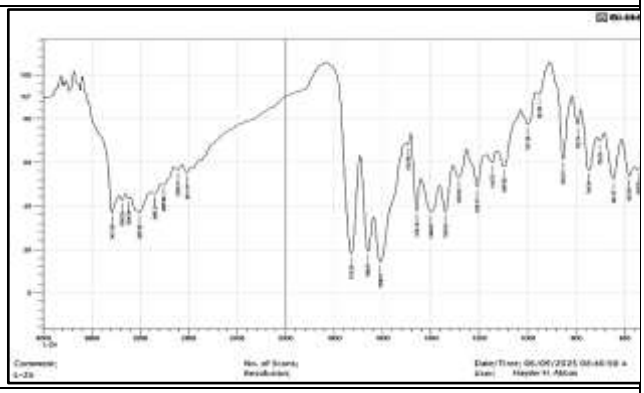
IR spectrum of ligand



IR spectrum of $[Co(L)_2Cl_2]$ Chelate complex



IR spectrum of $[Cu(L)_2Cl_2]$ Chelate complex



IR spectrum of $[Zn(L)_2Cl_2]$ Chelate complex

Figure 2. IR spectrum of ligand and its complexes

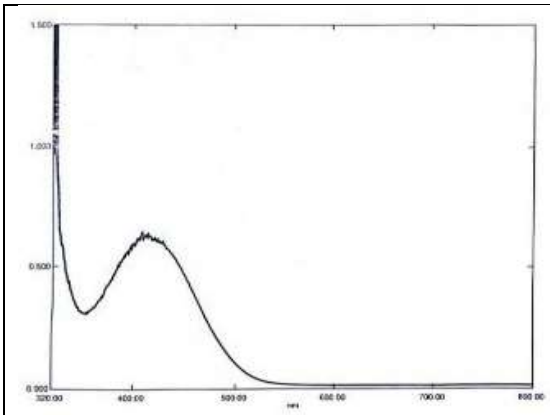
3.3. Electronic Spectra

The ligand's electronic spectra revealed that (n-π*) transitions were responsible for the highest absorption peak at a wavelength of 414 nm. Furthermore, (π-π*) transitions were identified as the cause of a peak at 300 nm [36,37]. The existence of double bonds with atoms that have non-bonding electron pairs (C=N), (C=O), and (C=C) groups in the ligand structures causes such transitions [38]. The electronic spectrum of the Co(II) complex exhibits penks at 678,615 as well as 457nm because of electronic transition type $^4T_{1g(F)} \rightarrow {}^4T_{2g(F)}$, $^4T1g(F) \rightarrow {}^4T1g(P)$, and $^4T_{1g(F)} \rightarrow {}^4A_{2g}$, respectively; other peaks at 372,311, 255, and 217nm due to ligand field and charge transfer. Octahedral geometry around the Cu (II) complex is indicated by the electronic spectrum [39], and the conductivity test value indicates that the complex is considered to be non-ionic. In addition, the electronic spectrum of the Cu(II) complex shows a peak at 454nm assigned to the electronic transition 2Eg→2T2g, while peaks at 352, 311, 231, and 217nm are attributed to ligand field and charge transfer. Furthermore, the electronic spectra indicate an octahedral geometry around the Cu(II) complex [40, 41], and the conductivity test indicates that the complex is non-ionic [42]. Along with the color

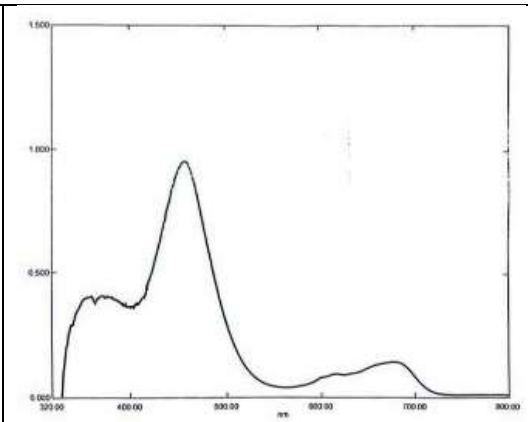
shift, a wavelength shift has been noted in the Zn(II) complex's electronic spectrum. Charge transfer transitions (M-L C.T.) were responsible for the complex's absorption peak at 428 nm. Because of the saturation of such orbitals with electrons (d10), the zinc complex's spectra have been characterized by the non-existence of electronic transitions of type (d-d). This result agrees well with earlier work on octahedral geometry [43, 44], and conductivity measurements indicate that it is a non-ionic compound. An octahedral structure was proposed for cobalt, copper, and zinc complexes based on the results.

Table 3. Molar conductance and electronic spectra of the ligand and the complexes

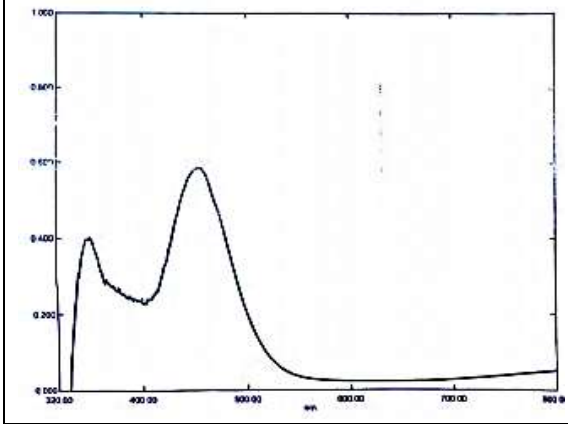
Compounds	**λ(nm)**	**Transition**	**ΛM ($S.cm^2.mol^{-1}$)**	**Geometry**	**Hybridization**
Ligand	414 300	n →π* π →π*	------	……	……
$[Co(L)_2Cl_2]$	678 615 457	$4T_1g(F) \rightarrow 4T_2g(F)$ $^4T_1g_{(F)} \rightarrow {}^4T_1g_{(P)}$ $^4T_1g_{(F)} \rightarrow {}^4A_2g$	2.33	Octahedral	Sp^3d^2
$[Cu(L)_2Cl_2]$	454	$2Eg \rightarrow 2T_2g$	2.97	Octahedral	Sp^3d^2
$[Zn(L)_2Cl_2]$	428	M-L, C.T.	2.64	Octahedral	Sp^3d^2



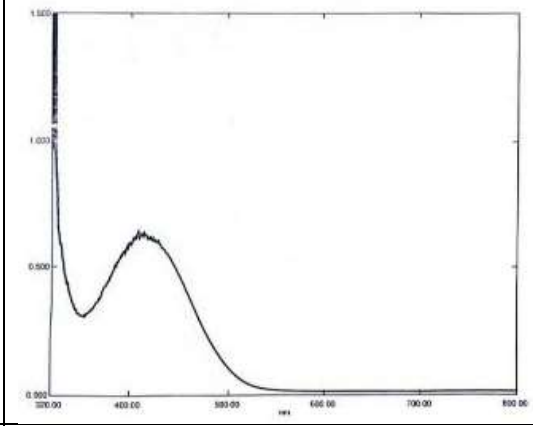
UV–Vis spectra of ligand



UV–Vis spectra of $[Co(L)_2Cl_2]$ Chelate complex



UV–Vis spectra of $[Cu(L)_2Cl_2]$ Chelate complex



UV–Vis spectra of of $[Zn(L)_2Cl_2]$ Chelate complex

Figure 3. Experimental UV–Vis absorption spectra of ligand and complexes

3.4. The $^{1H\ NMR}$ spectra of the ligand and Zn(II) complex

The ligand and Zn(II) complex 1H-NMR spectra, shown in Figures 7 and 8, respectively, were measured in d6-DMSO as the solvent using TMS as the internal reference and were distinguished by the presence of low-field signals. Furthermore, the free ligand's spectrum indicated the signal at (δ = 11.03ppm) attributed to the (NH) group, and the signal at (δ = 6.34-6.55, δ = 6.33-6.52) ppm is due to the (NH_2) group in ring[45]. The multiple signals of the aromatic protons appear in the (δ = 6.72-8.04, δ = 6.54-8.03) ppm range [46]. The solvent proton is responsible for a signal at (δ = 2.50-2.53) ppm [47]. Signal intensity differences between the Zn(II) complex as well as the free ligand are consistent with complex formation. [48].

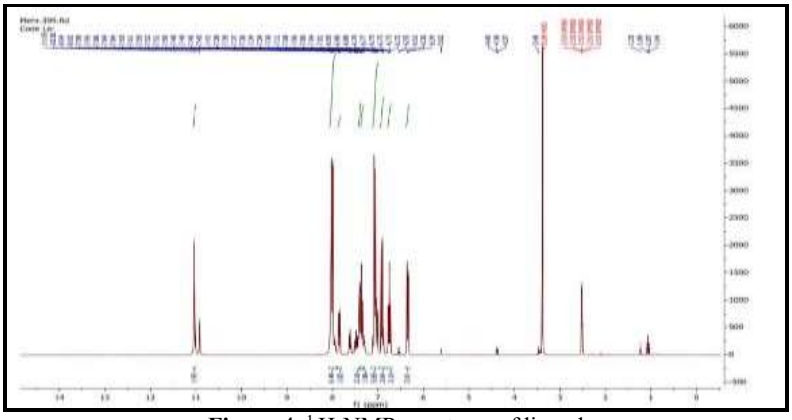


Figure 4. [1] H-NMR spectrum of ligand

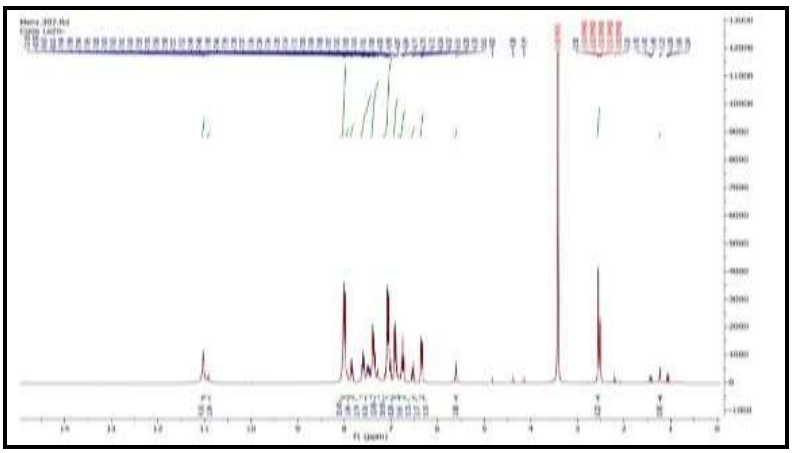


Figure 5. ^{1}H-NMR spectrum of $[Zn(L)_2Cl_2]$

3.5. The ^{13}C NMR Spectra of Schiff base ligand

Figure 9's ligand spectrum reveals resonance at (δ=168.113) ppm for the lactam and (δ=167.866) ppm for the carbon regarding the carbonyl amide group (C=O). A singlet signal for the carbon of the (-C=N) azomethine group at (δ = 163.790) ppm. Various signals at (δ=155.21, δ=153.722, δ=152.656, δ=147.598, δ=135.200, δ=131.101,δ=129.704, δ=128.501, δ=126. 010, δ=121.522, δ=117.453, and δ=111.380) ppm led to carbon atoms of aromatic rings and signal in δ=39.965ppm led into DMSO-d6 [49,50]**.** The ligand's ^{13}C NMR spectrum is presented in the paper, along with the corresponding proton assignments and chemical shifts (δ, ppm). Important details about the compound's functional groups and molecular structure are revealed in the study presented.

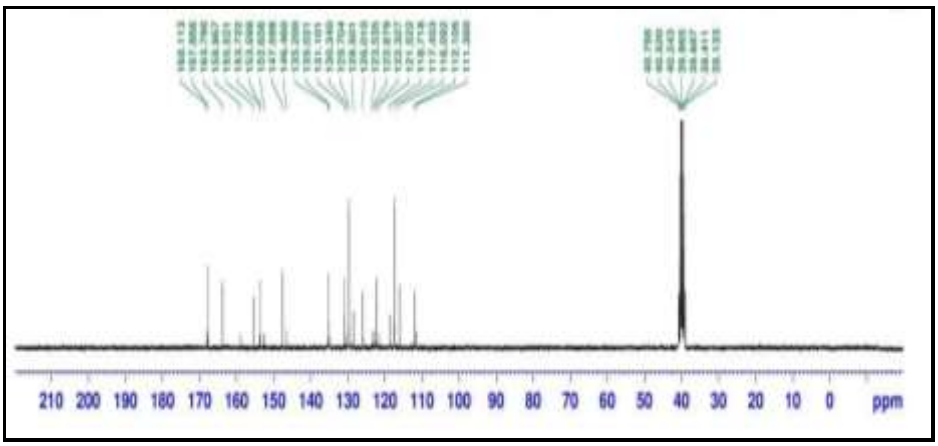


Figure 6. $^{13C\ NMR}$ spectrum of the ligand (L)

3.6. Conductivity measurement

The complexes' molar conductivities have been determined in DMSO solvent at a concentration of 1 in 10^{-3} molar at room temperature. For copper (II), cobalt (II), and zinc (II) complexes, the corresponding values were [2.97, 2.33, and 2.64] $mS.mol^{-1}$ cm^2. A comparison with the values in the table revealed the absence of ionic characteristics in all complexes, which corroborates the correct mixing ratio of ligand to metal ion (1:2). These findings support the proposed structural formula for the complexes and are consistent with existing literature[51] .

3.7. Anticancer activity

It has been investigated how the copper(II) complex [CuL_2Cl_2] affected the proliferation of normal cells (HDF) and colon cancer cell lines (HCT116). The highest inhibition rate for the copper (II) complex was 64.93% at a 600 µg/Ml concentration. In contrast, the highest inhibition rate for normal cells was 63.94% at the same concentration, as shown in Table 4-3. The findings indicated that the compound's concentration significantly influences the percentage of cell inhibition. Increasing the copper(II) complex concentration decreases cell viability, which increases the rate at which both normal and cancerous cells' growth is inhibited.

After 24 hours, the IC50 for HCT116 colon cancer cells was 264.76 µg/ml, which removed around half of the cells. This is less than the IC50 of 336.09 µg/ml for normal HDF colon cancer cells. This is encouraging, as it shows that [Cu(L)2Cl2] efficiently eliminates HCT116 colon cancer cells while having less impact on normal HDF cells. As shown in Figures 7 and 8 and Table 4 of the latest research [52], this discovery is critical for the possible use of such compounds as a good treatment for this type of cancer.

Table 4. With the use of a 24-hour MTT test at 37°C, the impact of the [Cu(L)2]Cl2 complex on the growth of colon cancer cell lines (HCT116) was compared with a normal cell line (HDF) at the same concentrations.

Con. ($\mu g.mL^{-1}$)	Mean Percentage (%) for every cell line			
	Cancerous line cells of HCT116		Normal line cells of HDF	
	Cell Viability	Cell Inhibition	Cell Viability	Cell Inhibition
7.4	93.04	6.96	93.00	7
22.22	84.56	15.44	86.36	13.64
66.66	71.48	28.52	76.00	24
200	56.29	43.71	60.64	39.36
600	35.07	64.93	36.36	63.64
	IC50 = 264.76 µg \ mL		IC50 = 366.09 µg/mL	

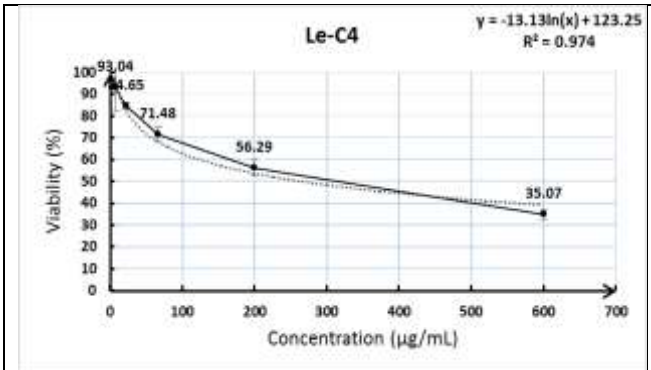


Figure 7. Percentage of viability in HCT116 Colon cancer cell line versus [$Cu(L)_2$]Cl_2 complex concentration.

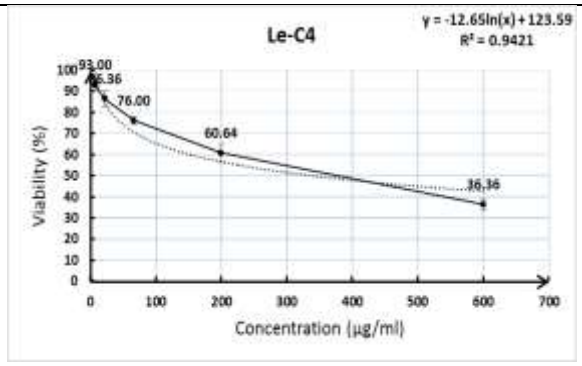


Figure 8. Percentage of viability in normal Colon cell line HDF versus [$Cu(L)_2$]Cl_2 complex concentration.

3.8. Computational methodology

Density Functional Theory (DFT) calculations were carried out using the Gaussian 9 software package [53-57]. The structure of the studied complex was first built and viewed in GaussView 9, then optimized without applying symmetry constraints. Two functionals, B3LYP [58] and ωB97XD [59], were used to assess the reliability of the optimized geometry and to obtain a more complete description of the interactions within the

complex. The optimizations were carried out using an effective core potential (ECP) with the LANL2DZ basis set [60] for Cu atoms, while the 6-31G** basis set [61] was used for the remaining atoms.

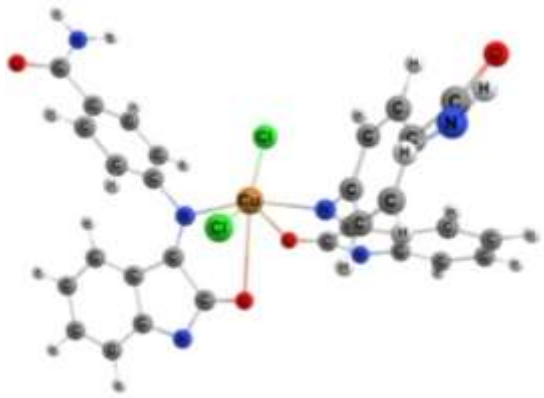
The frequency calculations were also done of the two methods and the calculated frequencies were all positive which indicates that the optimized structures are stable minima on the potential energy surface. Besides this, the ωB97XD functional was used to conduct Natural Bond Orbital (NBO) analysis to study charge transfer, donor acceptor interactions, as well as the electronic properties of the complex. GaussView 9 was used to perform the molecular visualization.

The optimized bond lengths of the copper complex were initially used to analyze the computational results. The comparison between B3LYP and ωB97XD provides a better understanding of the coordination environment around the copper center. This comparison can be used to assess the strength and nature of the Cu–N, Cu–Cl, and Cu–O interactions in the optimized structure. Table1. presents the calculated bond lengths of the copper complex using B3LYP and ωB97XD. The Cu–N bond showed only a small increase from 2.075 Å with B3LYP to 2.1064 Å with ωB97XD, while the Cu–Cl bond decreased slightly from 2.273 Å to 2.196 Å. This indicates that both methods give close results for the stronger coordination bonds around the copper center. The primary difference was in the Cu–O bonds. The Cu–O5 and Cu–O21 distances increased from 2.833Å using B3LYP to3.226 Å using ωB97XD. This is an indication that Cu–O interactions are weaker and more distant than the Cu–N and Cu–Cl bonds.

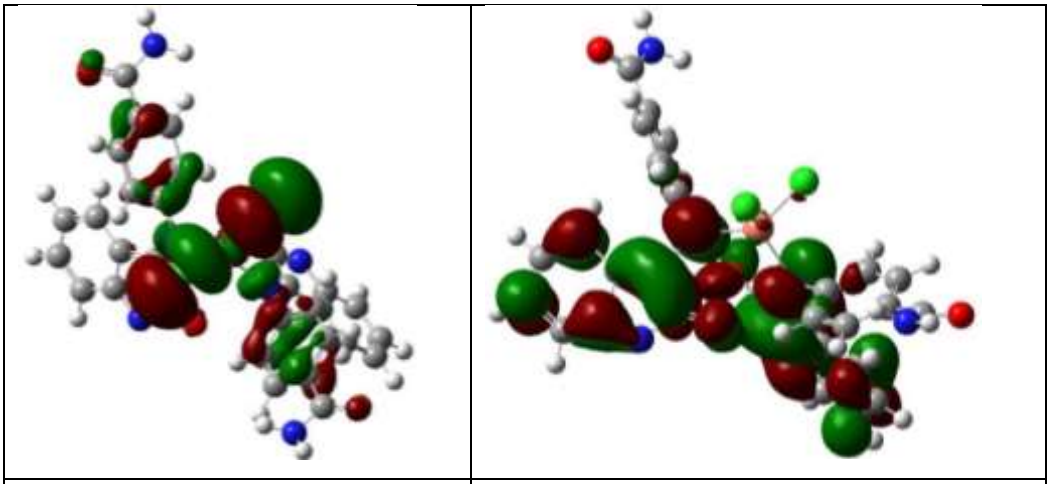
Table 5. Calculated bond lengths (Å) of the copper complex using B3LYP and ωB97XD methods

Methods	**Bond length**				
B3lyp	$Cu\text{-}N_4$	$Cu\text{-}N_{34}$	Cu-Cl	$Cu\text{-}O_5$	$Cu\text{-}O_{21}$
	2.075	2.0745	2.273	2.833	2.833
wB97XD	2.106	2.1059	2.1960	3.226	3.226

The difference between the two methods observed could be attributed to the treatment of the weak interactions by each functional. B3LYP is a popular and commonly used hybrid functional, and is not provided with an explicit dispersion correction, which can restrict its accuracy in describing weak coordination interactions. Conversely, ωB97X-D has long-range and dispersion corrections, which are more appropriate when weak interactions are involved, as in this case of the Cu–O interaction in this complex. Therefore, while both methods described the general coordination environment similarly, ωB97X-D provided a more reasonable description of the optimized structure and electronic behavior of the copper complex [58,59]. Furthermore, these optimized structural parameters perfectly align with and support the experimentally proposed hybridization.



Optimized structure



Homo	Lumo

Figure 9. Optimized structure and frontier molecular orbitals (HOMO = −0.319 a.u. and LUMO = −0.063 a.u.) of the copper complex calculated using the ωB97XD/6-31G** method.

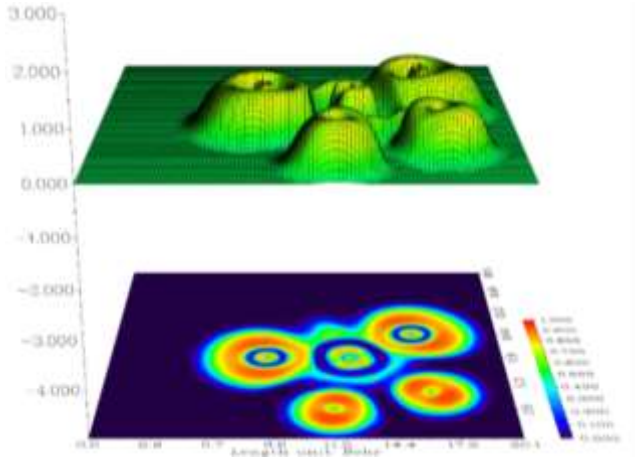


Figure 10. ELF surface and contour map of the copper complex obtained at the ωB97XD/6-31G** level of theory

The analysis of the copper complex using the combined HOMO-LUMO and ELF gives a straightforward insight into the electronic behavior of the complex [25,62]. The HOMO and LUMO distributions (Fig. 1) demonstrate the stable electronic structure, indicating donor-acceptor interactions around the coordination center. The relatively large HOMO–LUMO energy gap indicates good electronic stability and controlled charge-transfer behavior. In addition, the ELF maps in Fig. 2 confirm that the electron density is mainly localized around the coordinating donor atoms. These findings suggest that the complex may have promising physicochemical properties relevant to catalytic, adsorption, and functional material applications rather than purely biological activity [63,64].

As shown in Table 2, the NBO results highlight a clear shift in electron density within the copper complex. Specifically, the copper center holds a positive charge of +0.725, while the coordinating nitrogen and oxygen atoms carry negative charges. These values strongly suggest that the donor atoms are directing electrons toward the metal center. However, since NBO charges alone cannot definitively prove ligand-to-metal charge transfer (LMCT), we looked at the HOMO–LUMO and ELF analyses. Together, these tools give us a much clearer and more complete picture of how the complex coordinates and maintains its electronic stability.

Table 6. Natural Bond Orbital (NBO) charge distribution of the copper complex

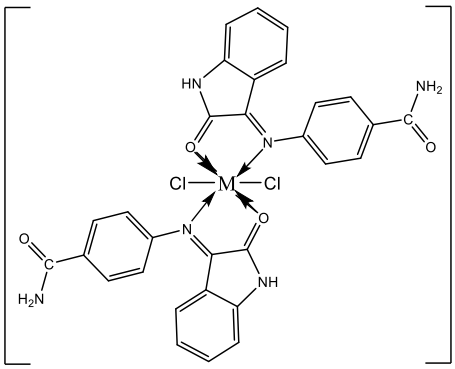
Metle	Cu	Cl	N	O
NBO charge	0.725	-0.507	-0.39to-0.88	-0.50to-0.63

Thus, the analysis of Natural Bond Orbital (NBO) charge suggests that the complex is stabilized by ligand-to-metal donor-acceptor interactions between the coordinating atoms of the ligand and the copper ion. So, the NBO charge analysis confirms that the complex is stabilized through ligand-to-metal donor-acceptor interactions between the coordinating atoms of the ligand and the copper ion. This e-stabilization directly supports the structural integrity and biological performance of the prepared copper complex. [65-67]

4. Conclusions

The synthesis, spectroscopic characterization, and metal complexes regarding a novel bidentate heterocyclic Schiff base ligand with Cu(II), Co(II), and Zn(II) metal ions are reported in the presented study. The isolated solid metal complexes have octahedral geometry (Figure 9). and have been characterized using current methods. The azomethine group nitrogen atom and the oxygen atom are coordinated to the ligand, giving a five-membered metal ring and acting as a bidentate ligand. The molar conductivity results show that complexes include chloride ions in the coordination ring and that metal complexes are non-electrolytes ,they were prepared with molar ratio of (1:2) [M:L] .The copper (II) complex was tested against human colon cancer (HCT116) and normal cell lines (HDF) as evidenced by IC50 and selectivity index (SI) values.

This study provides a basis for further investigation of the biological potential of the synthesized copper complex. The DFT calculations were useful in understanding the electronic characteristics of the prepared copper complex that complement its experimental characterization and support its biological evaluation.



M= Co(II) , ZN(II) and Cu(II)

Figure 11. The suggested structural formula of chelate complexes

References

1. Schiff, H., *Justus Liebigs Annalen der Chemie*. (1864). 131(1): p.p.118-119. https://doi.org/10.1002/jlac.18641310113.
2. Alredha, H.M., S.H. Ali, and Mohammed S.S. *Baghdad Science Journal*. (2022), 19(3): p. 0704-0704. http://dx.doi.org/10.21123/bsj.2022.19.3.0704
3. Raczuk, E., Samaszko F. J., Dmochowska B., and Madaj J. *Molecules*, (2022). 27(3): p.p. 787.
4. Bhattacharyya NK, Dutta D, Biswas J. A review on synthesis and biological activity of Schiff Bases. *Indian J Chem B*. (2021);60(11):1478-1489.
5. Al-Mulla, A review: Biological importance of heterocyclic compounds, *Der. Pharma. Chem.,* (2017),9(13), 141–147.
6. M.H. Hamzah, S. Eavani, E. Rafiee, $CoAl_2O_4/TiO_2$ nano composite as an anti-corrosion pigment, Mater Chem. Phys. 242 (2020) 122495. https://doi.org/10.1016/j.matchemphys.2019.122495

7. S.M. Alsafy, N.A. Alrazzak, Synthesis characterization and biological activity study of new heterocyclic compounds, Presented at the International Conference on Recent Advances in Science and Engineering (2023) Oct 4-5; Dubai, United Arab Emirates. https://doi.org/10.3390/engproc2023059178.
8. Liu Z, He W, Guo Z. Metal coordination in photoluminescent sensing. *Chem Soc Rev*. (2013);42(4):1568-1600.
9. E. Rafiee, M.H. Hamzah, S. Eavani, A novel NTiO2@CoAl2O4-H nanocomposite semiconductor: Study of electrochemical behavior and its relationship with photocatalytic performance, Optik., (2020) 203:163915. https://doi.org/10.1016/j.ijleo.2019.163915.
10. M. Sönmez, İ. Berber, E. Akbaş, Synthesis antibacterial and antifungal activity of some new pyridazinone metal complexes, Eur. J. Med. Chem., 41(1) (2006) 101–105.
11. A. Al-Ajili, S. Karim, Synthesis and characterization of new bis Schiff base derivatives based on adamantane and evaluation antioxidant activity, Eurasian Chem. Commun., 5(8) (2023). https://doi.org/10.22034/ecc.2023.395623.1630.
12. R. Katwal, H. Kaur, B.K. Kapur. Applications of copper—Schiff's base complexes: A review, Sci. Rev. Chem. Commun., 3 (2013) 1–15.
13. S.J. Hoseyni, M. Manoochehri, M.D. Asli, A novel Copper (II) Schiff base complex: Synthesis, characterization, and antibacterial activity, Chem. Res. Lett., 5(4) (2022) https://doi.org/10.22034/ crl.2022.168076.
14. R. Deo, C. Kumar, Synthesis and spectral characterization of binuclear compounds of Cu (II) and Ni (II) Schiff base of 2-Hydroxy-5-methylacetophenone and 1,2-Propylenediamine with alkali metal salts of trinitrophenol, J. Chem. Lett., 4(2) (2023). https://doi.org/10.22034/jchemlett.2023.389770.1109.
15. M.A. Phaniband, S.D. Dhumwad. Synthesis, characterization and biological studies of Co(II), Ni(II), Cu(II) and Zn(II) complexes of Schiff bases derived from 4-substituted carbostyrils [Quinolin-2(1H)-ones]. Trans. Met Chem. 32(8) (2007) 1117–1125. https://doi.org/10.1007/s11243-007-0295-2.
16. Tabassum, S., Zaki, M., Afzal, M. and Arjmand, F. (2013) Dalton Transactions. 42(27): p.p. 10029-10041. https://doi.org/10.1039/C3DT50646K**.**
17. Zampakou, M., Sofia Balala, Perdih F., Kalogiannis S., Turelc I. and P. George., RSC Advances. (2015). 5(16): p.p. 11861-11872. https://dio.org/10.1039/C4RA11682H.
18. Borreg, P., Cardenas, D., Ospina, F., Coy, E. and Quiroga, D., Journal of Fungi. (2023), 9(1): p.p. 113. https://doi.org/10.3390/jof9010113**.**
19. Al-Jumaili M., and Abid M., (2023), Tetrahedron Letters. 124: p.p. 154588.
20. Maldonado CR, Salassa L, Gómez-Blanco N, Mareque-Rivas JC. Nano-functionalization of metal complexes for molecular imaging and anticancer therapy. Coord Chem Rev. (2013);257(19-20):2668-2688.
21. Suzuki H, Kakigano T, Tada K, Igarashi M, Matsubara K, Inagaki A, Oshima M, Takao T (2005) Synthesis, structures, and reactions of coordinatively unsaturated trinuclear ruthenium polyhydrido complexes, {Ru(C5Me5)}3(μ-H)6 (Y = BF4, CF3SO3, 1/2(SO4), C6H5CO2, CH3CO2, B(C6H5)4, PF6) and [{Ru(C5Me5)}3(μ H)3(μ3-H)2]. Bull Chem Soc Jpn 78:67–87. https:// doi. org/ 10. 1246/ bcsj. 78. 67
22. Shima T, Sugimura Y, Suzuki H (2009) Heterometallic trinuclear polyhydrido complexes containing ruthenium and a group 9 metal, [Cp *3Ru2M(μ3-H)(μ-H) 3] (M = Ir or Rh; Cp* = η5-C 5Me5).
23. Lee C, Yang W, Parr RG (1988) Development of the Colle–Salvetti correlation-energy formula into a functional of the electron density. Phys Rev B 37:785–789. https:// doi. org/ 10. 1103/ PhysR evB. 37. 785
24. Perdew JP (1986) Density-functional approximation for the correlation energy of the inhomogeneous electron gas. Phys Rev B 33:8822–8824. https:// doi. org/ 10. 1103/ PhysR evB. 33. 8822
25. Yu, J., Hsu, C.-P., & Head-Gordon, M. (2022). Describing chemical reactivity with frontier molecular orbitals. *JACS Au, 2*(6), 1383–1394. **https://doi.org/10.1021/jacsau.2c00085**.
26. Gatti C, Lasi D (2007) Source function description of metal-metal bonding in d-block compounds. Faraday Discuss 135:55–78. https:// doi. org/ 10. 1039/ b6054 04h
27. Halim, S. A., El-Meligy, A. B., El-Nahas, A. M., & El-Demerdash, S. H. (2024). DFT study and natural bond orbital (NBO) population analysis of 2-(2-hydroxyphenyl)-1-azaazulene tautomers and their mercapto analogs. *Scientific Reports, 14*, 219. **https://doi.org/10.1038/s41598-023-50660-w** (Nature)
28. -Benesperi, I., Michaels, H., & Freitag, M. (2020). Copper coordination complexes for energy-relevant applications. *Energies, 13*(9), 2198. **https://doi.org/10.3390/en13092198**
29. R. Mahmoud, A. M. Hammam, S. A. El-Gyar, and S. A. Ibrahim; Monatshefte für Chemie., (1986),117, 313.
30. M. Ali, M. Hamzah, I. K. Jebur, and A. K. Ahmed, "Synthesis, Characterization and Biological Activity Evaluation of Some New Azo Derivatives from 2- Amino Benzothiazole and Their Derivatives," (KUJSS), (2018), vol. 13, no. 1, pp.212-227.
31. Gul, S., Maab, S., Rafiq, H., Alam, A., Rehman, M. U., Assad, M.,... & Khan, M. Exploring Bis-Schiff Bases with Thiobarbiturate Scaffold: In Vitro Urease Inhibition, Antioxidant Properties, and In Silico Studies. Russian Journal of Bioorganic Chemistry, (2024), 50(5), 1627-1638.
32. Hussein, K. A., Shaalan, N., & Faeq, M., Microwave-Assisted Preparation, Characterization, and Biological Activities of Schiff Bases Derived from 4-Aminoantipyrine with Acetonyl Acetone for Some New Rare-Earth Metals. Indonesian Journal of Chemistry, (2024), 24(5), 1470-1480.
33. Aljamali, N. M., Al-Zuhairi, A. J., Rasool, S. R., & Ameerghafil, R. A. Preparation of Organic Compounds by Microwave Technique with Applications. Journal of Modern Chemistry & Chemical Technology, (2025), 16(02), 2.

34. AL-Adilee, K. J. K., & Hassan, H. M., Preparation, Spectroscopic Characterization and Study of Biological Activity as Anticancer of Some Compounds Using A New Azo-Schiff Base Ligand (N, N, O) Derived From 2-amino-5-methyl Thiazol. International journal of health sciences, (2022),6(S4), 12002-12019.
35. Mermer, A., Tüzün, B., Daştan, S. D., & Çevik, Ö. Synthesis of novel Cu (II) complexes with N2O2 ligands: Characterization, theoretical calculations, antimicrobial, antioxidant, DNA binding, and in vitro anticancer activity studies. *Polyhedron*, (2023), 242, 116487.
36. Kumari, B., & Ahmad, K. Barbituric acid-derived azo dye metal complexes: Synthesis, characterization, DFT, and antimicrobial analysis: Applied Organometallic Chemistry, (2024), 38(7), e7525.
37. Jirjees, V. Y., & Al–Hamdani, A. A. S. Synthesis, characterization and evaluation of anticancer and antioxidant activity of new azo dye derivatives from tryptamine and complexes. Bulletin of the Chemical Society of Ethiopia, **(2025),** 39(7), 1317-1334.
38. Zhao, H. N., Hu, X., Tian, Z., Gonzalez, M., Rideout, C. A., Peter, K. T.,... Kolodziej, E. P., Transformation products of the tire-rubber antioxidant 6PPD in heterogeneous gas-phase ozonation: identification and environmental occurrence. Environmental Science & Technology, (2023), 57(14), 5621- 5632.
39. Saeed, F. T., & Jasim, Z. U., Synthesis and characterization of new mn (ii), co (ii), ni (ii), cu (ii), zn (ii) and cd (ii) complexes with [(z)-3 ((6-aminopyridine-2-yl) imino) indolin-2-one] ligand. *Kimya Problemleri* (2024), *22*(1), 103-114.
40. A.B.P. Lever, Inorganic Electronic Spectroscopy, Elsevier, Amsterdam, 395 (1968); C. K. Jorgenson, Acta Chem., Scand. Nutal and D. W. A. Sharp, J. Inorg. Nucl. Chem., (1964), 26: 1895.
41. Noor, S. S., & Kareem, I. K., A bio-scientific study of the new gold complex as an anti -breast cancer agent, as well as its preparation, Molar Conductivity, and Spectral identification of some other metal complexes—Journal *of Kufa for Chemical Sciences*, (2024), *3*(3), 201- 222.
42. J.J. Rios, M.C. Reico and A. Vllar, "Antimicrobial screening of natural products", J.Enth.Pharmace, (1988),l23,127-149.
43. Kurdy, R. N., & Kareem, I. K., Synthesis, Characterization and study of molecular docking of a new Azo-Schiff base ligand with its metal complexes. *Journal of Kufa for Chemical Sciences*, (2024), *3*(3), 68-85.
44. Hilal, T. A. A., & Kareem, I. K., Synthesis of some metal complexes with new heterocyclic ligand (5-(((2-(3-(1 h-indol-3-yl) acryloyl) phenyl) amino) methylene)-2-thiooxodihydropyrimidine-4, 6 (1 h, 5 h)-dione) and their biological effectiveness as antioxidant and anti-cancer. Indones. J. Chem, (2024) 10, 20-130.
45. TUSHAR S. U., SANJAY K. P. and JYOTSNA G. P, Co(II), Ni(II), Cu(II) and Zn(II) Metal Complexes of Hydrazone Schiff Base Ligand:Synthesis, Characterization, Thermal Behavior, Antioxidant and Antimicrobial Studies. Asian Journal of Chemistry; (2024). Vol. 36, No. 8, 1781-1792.
46. Jawad, S. H., & Al-Adilee, K. J., Synthesis, spectroscopic characterization and biological activities as an anticancer and antioxidant of the Pd (II) and Pt (IV) complexes with a new azo dye ligand derived from 5-methyl imidazole. *Journal of Molecular Structure*, (2023), *1277*, 134846. 206-
47. Bashandy,M.S.,Mohamed,F.A.,El-Molla,M.M.,Sheier,M.B. and Bedair,A.H. Open.J.Med.Chem, (2016),6,18-35.
48. Schuur JH, Selzer P, Gasteiger J. The coding of the three-dimensional structure of molecules by molecular transforms and its application to structure-spectra correlations and studies of biological activity. J Chem Inf Comput Sci. (1996),36(2):334-344.
49. G. Mishra, P. K. Dwivedi, N. Verma, S. Srivastava, and A. K. Singh, "Copper Nitrate Catalyzed Synthesis Of Novel Thiazolyl Hydrazones: Anti-Inflammatory Effect Via COX-2 / IL-6 Dual Antagonistic Action," Journal Pharm. Negat. Results, vol. (2022),13, no. 10, pp. 3821–3833.
50. Al-Hamdani, A. A.S, Balkhi, A. M, Falah, A, Shaker, Sh. A. J. Chil. Chem. Soc.(2015), 60 (1): 2774-2785.
51. W. J. Geary; *Coord Chem Rev*, (1971), 7, 81.
52. Unavane, S., Patil, R., Syed, S., & Jain, H. K.. Exploring the therapeutic potential of copper and cobalt complexes as anticancer agents: a comprehensive review. Transition Metal Chemistry, (2025), 50(4), 407-430.
53. Frisch, M. J.; Trucks, G. W.; Schlegel, H. B.; Scuseria, G. E.; Robb, M. A.; Cheeseman, J. R.; Scalmani, G.; Barone, V.; Mennucci, B.; Petersson, G. A.; Nakatsuji, H.; Caricato, M.; Li, X.; Hratchian, H. P.; Izmaylov, A. F.; Bloino, J.; Zheng, G.; So DJ (2013) Gaussian 09 Revision D. 01 Release Notes. Gaussian, Inc, Wallingford CT (June):1–13.
54. Kadhim NH, Hussain T, Abdulhussein HA (2025) Gallium doped AlP monolayers: A promising architecture for gas sensing. Comput Theor Chem 115301.
55. Kadhim NH, Abo Nasria AH, Alhameedi K, Hussain T, Abdulhussein HA (2025) Light Transition Metal Functionalized ψ-Graphene as Promising Hydrogen Storage Architecture. Advanced Energy and Sustainability Research 2500154.
56. Hussein MA, Al-Ameed K, Almansori AK, Owaid NJ (2024) Efficient amide bond formation via tropylium ion organocatalysis. RSC Adv 14(46):34428–34434
57. Mohammed MA, Abdulhussein HA, Al-ibadi MAM, Raju RK, Johnston RL (2021) Global minima and structural properties of AuFe nanoalloys from a Mexican Enhanced Genetic Algorithm-based Density Functional Theory. Chem Phys Lett 776:138675.
58. becke, A. D. (1993). Density-functional thermochemistry. III. The role of exact exchange. The Journal of Chemical Physics, *98*(7), 5648–5652. https://doi.org/10.1063/1.464913.

59. Da CJ, Head-Gordon M (2008) Long-range corrected hybrid density functionals with damped atom-atom dispersion corrections. Phys Chem Chem Phys 10:6615–6620. https:// doi. org/ 10. 1039/ b8101 89b
60. Fuentealba P, Preuss H, Stoll H, Von Szentpály L (1982) A proper account ocore-polarization with pseudopotentials: single valence-electron alkali compounds. Chem Phys Lett 89:418–422. https:// doi. org/ 10. 1016/ 0009- 2614(82) 80012-2
61. Hehre WJ, Ditchfield K, Pople JA (1972) Self-consistent molecu lar orbital methods. XII. Further extensions of Gaussian-type basis sets for use in molecular orbital studies of organic molecules. J Chem Phys 56:2257–2261. https:// doi. org/ 10. 1063/1. 16775 27
62. Lindmaa, A., Davidsson, J., Mattsson, A. E., & Armiento, R. (2019). Semi-local parameterization of the electron localization function in second-order density gradients. *Physical Review B, 100*(14), 144112. https://doi.org/10.1103/PhysRevB.100.144112
63. Savin, A., Nesper, R., Wengert, S., & Fässler, T. F. (1997). ELF: The electron localization function. *Angewandte Chemie International Edition in English, 36*(17), 1808–1832. https://doi.org/10.1002/anie.199718081
64. Benesperi, I., Michaels, H., & Freitag, M. (2020). Copper coordination complexes for energy-relevant applications. *Energies, 13*(9), 2198. https://doi.org/10.3390/en13092198
65. Reed, A. E., Curtiss, L. A., & Weinhold, F. (1988). Intermolecular interactions from a natural bond orbital, donor–acceptor viewpoint. *Chemical Reviews, 88*(6), 899–926. https://doi.org/10.1021/cr00088a005
66. Weinhold, F. (1998). Natural bond orbital methods. In P. von R. Schleyer, N. L. Allinger, T. Clark, J. Gasteiger, P. A. Kollman, H. F. Schaefer III, & P. R. Schreiner (Eds.), *Encyclopedia of Computational Chemistry* (Vol. 3, pp. 1792–1811). Wiley.
67. Halim, S. A., El-Meligy, A. B., El-Nahas, A. M., & El-Demerdash, S. H. (2024). DFT study, and natural bond orbital (NBO) population analysis of 2-(2-hydroxyphenyl)-1-azaazulene tautomers and their mercapto analogues. *Scientific Reports, 14*, 219. https://doi.org/10.1038/s41598-023-50660-w.